Hubble Space Telescope

Cycle 16 GO Proposal

Decelerating and Dustfree: Efficient Dark Energy Studies with Supernovae and Clusters

Principal Investigator: Prof. Saul Perlmutter

Institution: University of California - Berkeley

Electronic Mail: saul@lbl.gov

Scientific Category: COSMOLOGY

Scientific Keywords: COSMOLOGICAL PARAMETERS AND DISTANCE SCALE, CLUSTERS OF GALAXIES, SUPERNOVAE, GRAVITATIONAL LENSING

Instruments: ACS, NICMOS

Proprietary Period: 12

Orbit Request	Prime	Parallel
Cycle 16	234	28

Abstract

Our cycle 14 program has demonstrated a new, extremely efficient approach to obtain z>1 dust-free Type Ia supernovae, and we propose to capitalize on this new technique. We will collect a total sample of ~20 z>1 SNeIa in cluster elliptical galaxies, each of which will carry the weight of up to 10 color-corrected z>1 SNe hosted by spiral galaxies. We will further boost our efficiency by including new, more massive, z>1 clusters and by further reducing the measurement error on each SN. The measurement will yield dark energy constraints that do not suffer from the major systematic and statistical uncertainty at these redshifts, that of extinction correction. By targeting massive galaxy clusters at z>1, we probe a unique and well-understood host galaxy environment, and obtain five-times higher efficiency than a survey of random fields in detection of Ia supernovae in elliptical galaxies. The data will make possible a factor of two improvement on supernova constraints on dark energy time evolution and a much larger improvement on systematic uncertainty. Via weak lensing, these same deep cluster images also yield fundamental mass calibrations required for ongoing and future studies which aim to measure dark energy using the evolution of cluster abundances, as well as a rich program of cluster studies. We will obtain both a cluster dataset and a SN Ia dataset that will be a longstanding scientific resource.

Investigators:

	Investigator	Institution	Country
PI	Prof. Saul Perlmutter	University of California - Berkeley	USA/CA
CoI	Dr. Greg Aldering	Lawrence Berkeley National Laboratory	USA/CA
CoI	Dr. Rahman Amanullah	University of California - Berkeley	USA/CA
CoI	Mr. Kyle Barbary	University of California - Berkeley	USA/CA
CoI	Prof. L Felipe Barrientos	Universidad Catolica de Chile	Chile
CoI	Dr. Mark Brodwin	Jet Propulsion Laboratory	USA/CA
CoI&	Dr. Kyle Dawson	Lawrence Berkeley National Laboratory	USA/CA
CoI	Dr. Arjun Dey	National Optical Astronomy Observatories, AURA	USA/AZ
CoI	Prof. Mamoru Doi	University of Tokyo, Institute of Astronomy	Japan
CoI	Prof. Megan Donahue	Michigan State University	USA/MI
CoI	Dr. Peter Eisenhardt	Jet Propulsion Laboratory	USA/CA
CoI	Prof. Erica Ellingson	University of Colorado at Boulder	USA/CO
CoI	Dr. Andrew S. Fruchter	Space Telescope Science Institute	USA/MD
CoI	Dr. David Gilbank	University of Toronto	Canada
CoI	Prof. Michael D. Gladders	University of Chicago	USA/IL
CoI	Prof. Gerson Goldhaber	Lawrence Berkeley National Laboratory	USA/CA
CoI	Prof. Anthony H. Gonzalez	University of Florida	USA/FL
CoI	Dr. Buell T. Jannuzi	National Optical Astronomy Observatories, AURA	USA/AZ
CoI*	Prof. Ariel Goobar	Stockholm University	Sweden
CoI	Dr. Joseph Hennawi	University of California - Berkeley	USA/CA
CoI	Prof. Henk Hoekstra	University of Victoria	Canada
CoI	Dr. David Johnston	Jet Propulsion Laboratory	USA/CA
CoI	Dr. Nobunari Kashikawa	National Astronomical Observatory of Japan (NAOJ)	Japan
CoI	Dr. Benjamin Koester	University of Chicago	USA/IL
CoI	Dr. Natalia Kuznetsova	Lawrence Berkeley National Laboratory	USA/CA
CoI*	Dr. Christopher Lidman	European Southern Observatory - Chile	Chile
CoI	Dr. Eric Linder	Lawrence Berkeley National Laboratory	USA/CA
CoI	Prof. Lori M. Lubin	University of California - Davis	USA/CA
CoI	Mr. Joshua Meyers	University of California - Berkeley	USA/CA
CoI*	Dr. Ramon Miquel	Universidad de Barcelona	Spain
CoI	Dr. Tomoki Morokuma	University of Tokyo, Institute of Astronomy	Japan

	Investigator	Institution	Country
CoI	Dr. Christopher Mullis	University of Michigan	USA/MI
CoI	Dr. Nino Panagia	Space Telescope Science Institute	USA/MD
CoI	Dr. Marc Postman	Space Telescope Science Institute	USA/MD
CoI	Dr. Jason Rhodes	Jet Propulsion Laboratory	USA/CA
CoI*	Dr. Piero Rosati	European Southern Observatory - Germany	Germany
CoI	Mr. David Rubin	University of California - Berkeley	USA/CA
CoI	Dr. David J. Schlegel	Lawrence Berkeley National Laboratory	USA/CA
CoI	Dr. Anthony L. Spadafora	Lawrence Berkeley National Laboratory	USA/CA
CoI	Dr. S. Adam Stanford	University of California - Davis	USA/CA
CoI*	Dr. Vallery Stanishev	Stockholm University	Sweden
CoI	Dr. Daniel Stern	Jet Propulsion Laboratory	USA/CA
CoI	Dr. Nao Suzuki	Lawrence Berkeley National Laboratory	USA/CA
CoI	Prof. Lifan Wang	Texas A & M Research Foundation	USA/TX
CoI	Dr. Naoki Yasuda	University of Tokyo, Institute of Cosmic Ray Research	Japan
CoI	Prof. Howard K. Yee	University of Toronto	Canada

Number of investigators: 46

* ESA investigators: 5

& Contact CoI: Dr. Kyle Dawson

Target Summary: [Names and coords excised here, but not in the submitted proposal!]

Target	RA	Dec	Magnitude
ISCS14	14	+32	V = 25.0
1012.28	14	+34	V = 25.0
1012.52	14	+33	V = 25.0
1113.7.7	14	+34	V = 25.0
ISCS14	14	+32	V = 25.0
13	14	+34	V = 25.0
ISCS14	14	+33	V = 25.0
ISCS14	14	+33	V = 25.0
IRAC02	02	-04	V = 25.0
RCS02	02	-03	V = 25.0
RCS02	02	-03	V = 25.0

Target	RA	Dec	Magnitude
RCS03	03	-28	V = 25.0
RCS04	04	-29	V = 25.0
RCS15	15	+09	V = 25.0
RCS21	21	-04	V = 25.0
RCS23	23	+00	V = 25.0
RCS23	23	-36	V = 25.0
RDCS08	08	+44	V = 25.0
RDCS12	12	-29	V = 25.0
XMM22	21	-17	V = 25.0
XMMUJ22	22	-25	V = 25.0
XMMUJ12	12	+01	V = 25.0
CL16	16	+43	V = 25.0
RDCS09	09	+54	V = 25.0
RCS1	02	-03	V = 25.0
RCS2	03	-28	V = 25.0
RCS3	04	-29	V = 25.0
TOO-SN-11ORB	14	+32	V = 25.0
TOO-SN-2ORB	08	+44	V = 25.0
TOO-SN-1ORB	12	-29	V = 25.0

Observing Summary:

Target	Config Mode and Spectral Elements	Flags	Orbits
ISCS14	ACS/WFC Imaging F850LP		8 (1x8
	ACS/WFC Imaging F775W		
10	ACS/WFC Imaging F850LP		8 (1x8
	ACS/WFC Imaging F775W		
10	ACS/WFC Imaging F850LP		8 (1x8
	ACS/WFC Imaging F775W		
11	ACS/WFC Imaging F850LP		8 (1x8
	ACS/WFC Imaging F775W		
ISCS14	ACS/WFC Imaging F850LP		9 (1x9
	ACS/WFC Imaging F775W		

Target	Config Mode and Spectral Elements	Flags	Orbits
13	ACS/WFC Imaging F850LP		9 (1x9)
	ACS/WFC Imaging F775W		
ISCS14	ACS/WFC Imaging F850LP		9 (1x9)
ISCS14	ACS/WFC Imaging F850LP		9 (1x9)
	ACS/WFC Imaging F775W		
IRAC02	ACS/WFC Imaging F850LP		8 (1x8)
	ACS/WFC Imaging F775W		
RCS02	ACS/WFC Imaging F850LP		8 (1x8)
	ACS/WFC Imaging F775W		
RCS02	ACS/WFC Imaging F850LP		8 (1x8)
	ACS/WFC Imaging F775W		
RCS03	ACS/WFC Imaging F850LP		8 (1x8)
	ACS/WFC Imaging F775W		
RCS04	ACS/WFC Imaging F850LP		7 (1x7)
	ACS/WFC Imaging F775W		
RCS15	ACS/WFC Imaging F850LP		7 (1x7)
	ACS/WFC Imaging F775W		
RCS21	ACS/WFC Imaging F850LP		7 (1x7)
	ACS/WFC Imaging F775W		
RCS23	ACS/WFC Imaging F850LP		7 (1x7)
	ACS/WFC Imaging F775W		
RCS23	ACS/WFC Imaging F850LP		7 (1x7)
	ACS/WFC Imaging F775W		
RDCS08	ACS/WFC Imaging F850LP		7 (1x7)
	ACS/WFC Imaging F775W		
RDCS12	ACS/WFC Imaging F850LP		7 (1x7)
	ACS/WFC Imaging F775W		
XMM22	ACS/WFC Imaging F850LP		7 (1x7)
	ACS/WFC Imaging F775W		
XMMUJ22	ACS/WFC Imaging F850LP		7 (1x7)
	ACS/WFC Imaging F775W		
XMMUJ12	ACS/WFC Imaging F850LP		7 (1x7)
	ACS/WFC Imaging F775W		
CL16	ACS/WFC Imaging F850LP		8 (1x8)

Target	Config Mode and Spectral Elements	Flags	Orbits
	ACS/WFC Imaging F775W		
RDCS09	ACS/WFC Imaging F850LP		7 (1x7)
	ACS/WFC Imaging F775W		
RCS1	ACS/WFC Imaging F850LP		7 (1x7)
	ACS/WFC Imaging F775W		
RCS2	ACS/WFC Imaging F850LP		7 (1x7)
	ACS/WFC Imaging F775W		
RCS3	ACS/WFC Imaging F850LP		7 (1x7)
	ACS/WFC Imaging F775W		
TOO-SN-11ORB	NIC2 Imaging F110W	TOO	14 (7x2)
TOO-SN-2ORB	NIC2 Imaging F110W	TOO	4 (2x2)
TOO-SN-1ORB	NIC2 Imaging F110W	TOO	10 (1x10)
TOO-SN-11ORB	ACS/WFC Imaging F850LP	CPAR, TOO	14 (7x2)
TOO-SN-2ORB	ACS/WFC Imaging F850LP	CPAR, TOO	4 (2x2)
TOO-SN-1ORB	ACS/WFC Imaging F850LP	CPAR, TOO	10 (1x10)

Total prime orbits: 234

Total coordinated parallel orbits: 28

Scientific Justification

Using Type Ia Supernovae in Cluster Ellipticals to Measure Cosmology

Striking results from the HST Cycle 14 program we just completed in December open up a new approach to one of the key cosmology goals of this decade: the detailed, accurate measurement of the universe's expansion history, from deceleration through acceleration, to study the dark energy. There is currently only one tool in use for this measurement, the type Ia supernova (SN Ia) luminosity distance, and only HST SN observations can provide the required signal-to-noise ratio at $z > 1$ where the critical transition from acceleration to deceleration becomes evident. However, at these redshifts even the HST's statistical strength is badly compromised by large uncertainties in the host-galaxy-dust extinction correction. More importantly, the known scatter and any evolution of the dust's extinction law (R_B) introduces large systematic errors. Extinction is thus the dominant uncertainty at these redshifts. Our new HST results show that we can solve these problems by finding SNe Ia in $z > 1$ cluster ellipticals – a very efficient use of HST. We can then select and test for a population that is specifically dust-free, and create a new $z > 1$ Hubble diagram with dramatically stronger statistical and systematic significance.

What did our just-completed program demonstrate? (1) We had proposed that by searching in rich galaxy clusters we could double the number of $z > 1$ SNe discovered in each ACS field, and obtain an even greater enhancement of the number of SNe in elliptical hosts. Figure 1a shows that the method is a success on both counts: the ten new elliptical hosted SNe are primarily the result of searching in clusters. (2) We had proposed that cluster ellipticals would provide a testably dust-free environment, so their SNe would exhibit a much tighter magnitude dispersion without extinction correction than the SNe in later-type galaxy hosts with or without extinction correction. Figure 1b shows that this expectation has been more than fulfilled: the dispersion of *measured* scatter about the Hubble line is even narrower than we had hoped for, $\sigma = 0.09$ mag – so narrow, in fact, that it is now dominated by the photon noise, and it is possible that these SNe are even a better standard candle. Each of these SNe is thus worth more than 10 SNe in non-elliptical environments at $z \gtrsim 1$, based on their measured dispersion (see below).

This proposal: Recent work with 23 SNe Ia in this redshift range but without cluster searching has been presented as evidence for dark energy effects above z = 1 (Riess et al. 2007), but the error bars have been large enough that the data could equally well be taken as inconclusive and it is matched by the error bar from even the first few cluster-elliptical SNe we found in Cycle 14 (see Figures 1b and 2). We here propose to collect a much more significant sample of $\sim$24 elliptical-hosted SNe Ia ($\sim$18 in clusters), each with a higher signal-to-noise ratio to match their small intrinsic dispersion, to provide new stronger and unbiased constraints on the dark energy at the $z > 1$ epochs. This sample will have the same number of SNe Ia as in Riess et al. 2007, but with statistical strength equivalent to $\sim$200 later-type-host SNe. This new $z > 1$ dust-free Hubble diagram with 18 cluster-elliptical-host SNe Ia would thus provide a first constraint at the $\sim$0.02 mag level that can distinguish between theories of dark energy with time-varying w that are indistinguishable with the best lower redshift data expected from the SNLS and ESSENCE projects (see Figure 2a). More important is that if this new "dust-free" $z > 1$ Hubble diagram shows surprising dark energy behavior it will not be dismissable as an artifact of dust-correction

systematics. Figure 2a also shows that, because of these systematics, this is a goal that cannot be reached by adding to the existing *non*-elliptical Hubble diagram, even if an additional ∼600 orbits were spent to double the sample size. The proposed cluster-elliptical-only sample will also be large enough to be used together with the large, well-measured CFHT Legacy Survey and ESSENCE final samples of elliptical hosted SNe at $z \lesssim 0.8$, together yielding the strong constraints on w vs. w' shown in Fig. 2c — without extinction systematics.

Using the images we have collected so far for the most massive of our high-redshift clusters allows us not only to start the new proposed search with extremely deep reference images for half of our sample, but also to double the exposure depth for these clusters with two filters, F775W and F850LP, enabling a major step forward in the cluster science and other cosmological measurement techniques. In particular, counting clusters is an extremely sensitive measure of expansion history (and dark energy), if their masses can be estimated with reasonable precision. By replacing our least rich half of the clusters with newly discovered rich clusters, and with the addition of deep F775W data, we propose to study cluster masses via weak lensing from the same HST images, and calibrate Sunyaev-Zeldovich/X-Ray measurements to those same clusters.

How problematic is the extinction correction uncertainty at $z \gtrsim 1$? The correction for extinction from dust in the host galaxies is currently the single dominant source of both statistical and systematic error for SNe distances and the derived cosmological parameters – dramatically so at $z > 1$ even with HST (see Figure 1b). The typical color uncertainty for HST-studied $z > 1$ SNe is 0.05 – 0.1 in $B - V$, leading to uncertainties in extinction correction of as high as ∼0.4 mag! This dispersion grows worse – and an additional systematic uncertainty is introduced – after accounting for dispersion and drifts in intrinsic color and the dust reddening coefficient, $R_B \equiv A_B/E(B-V)$, which Draine (2003) notes can vary from the fiducial value 4.1 by ± 0.5 and for which empirical studies of multiband SNe colors indicate an even wider range. (The actual dispersion about the Hubble-line fit for $z > 1$ SNe Ia corrected for extinction matches the 0.4 mag value, even before accounting for these additional systematics.) Figure 2b shows the resulting poor constraints on the dark-energy equation-of-state parameter and its time variation, w_0 vs. w'. These constraints are insufficient to distinguish between almost any current dark energy model.

To correct for dust extinction, either one needs exquisitely good multi-band color information, or one is driven to use a Bayesian prior on $a)$ the mean and probability distribution of R_B and $b)$ the probability distribution of the amount of dust. (This is the approach taken by Riess et al. 2007 to reduce the dispersion to 0.36 mag, or 0.26 mag after rejecting the largest deviant.) If even just one of these priors is redshift dependent, the final result will be systematically biased. The effect of varying R_B can be seen in Fig. 2b as the difference between the three open contours. If aggressive Bayesian priors are chosen, the larger systematic errors outweigh the smaller statistical errors.

How is this problem solved using SNe Ia in cluster ellipticals? In Sullivan et al. (2003), we found that the dispersion (including ground-based measurement error) about the Hubble diagram out to $z \sim 0.5$ for elliptical-hosted SNe is 0.16 mag. Even lower measured dispersion for elliptical-hosted SNe has since been confirmed with better photometry, both at the low redshifts, $z < 0.1$, where Jha et al. (2007) finds $\sigma = 0.11$ mag and over the high-redshift range, $0.2 < z < 0.8$, where a preliminary study of 40 SNe from the CFHT SN Legacy Survey (Sullivan 2006) finds $\sigma = 0.14$ mag (even including significant measurement noise). At still higher redshifts, our just-completed

HST program SNe show $\sigma = 0.09$ mag in a preliminary analysis. This is more than four times smaller than just the measurement uncertainty for extinction-corrected SNe Ia at $z > 1$ and three times smaller than achieved by even the most agressive Bayesian prior on dust — primarily due to the absence of dust to correct for. Thus, each elliptical SNe Ia is statistically worth more than 10 SNe Ia in spirals when making cosmological measurements – and without the aforementioned systematics associated with extinction correction.

At $z > 1$, why is it then important to study elliptical-hosted SNe specifically in clusters? Although evidence for dust is found in $\sim 50\%$ of nearby ellipticals, the quantity of dust is generally very small and confined to the central few hundred pc (e.g. Tran et al. 2001). Recent Spitzer data (Temi et al. 2005) confirms that most nearby ellipticals have the SED's expected for dust-free systems. Field ellipticals at larger redshifts do show signs of increasing star-formation in that blue clumps have been detected in nearly 50 % of them at $z \sim 1$ (Pasquali et al. 2006), but blue clumps are *not* found in cluster ellipticals at $z \sim 1$. Thus it is ideal to use cluster-elliptical-hosted SNe at these very high redshifts to avoid the possibility of any dust. That said, the vast majority of individual $z > 1$ field-elliptical-hosted SNe may prove to be similarly unaffected by dust. We see evidence for this in that our three $z > 1$ field-elliptical-hosted SNe show a similarly low dispersion to the cluster-elliptical hosted SNe. This small sample is encouraging, but inconclusive: Riess et al. (2007) reported a higher dispersion, $\sigma = 0.25$ mag, for the four $z \gtrsim 1$ field-elliptical-hosted SNe observed within 20 days of peak in HST blank field surveys. However, these should be treated with caution since two of these are noted to have worst-case host galaxy subtraction (on core), and a third has a poorly constrained lightcurve shape. Thus, while field-elliptical-hosted SNe *may* indeed prove to be similarly useful (an idea we will be able to test with the proposed increased statistics), cluster ellipticals are the most reliable, best understood environment.

A key advantage to using SNe in cluster elliptical hosts is that they can be tested individually for dust. This is because the clearest evidence that dust has little effect on stars in cluster elliptical galaxies comes from the tightness of their color-magnitude relations. The dispersion in the colors of early-type galaxies is very small in clusters ranging from Coma to intermediate redshifts (Bower et al. 1992; Ellis et al. 1997; Stanford, Eisenhardt & Dickinson 1998; van Dokkum et al. 2001). In fact, this relation has been shown by Hogg et al. (2004) to be universal for early-type galaxies in clusters and in lower-density environments using an enormous sample from SDSS. Results from ACS imaging show the same strikingly small dispersion in color extends to redshifts $z \gtrsim 1$ (Figure 3a). ACS imaging of RDCS1252-29 at $z = 1.24$ by Blakeslee et al. (2003) found an intrinsic dispersion of 0.024 ± 0.008 mag for 30 ellipticals in the F775W - F850LP color, which approximates rest-frame $U - B$. This dispersion is comparable to that found by Bower et al. in Coma. Since some intrinsic color variation in the age and metallicity of stellar populations of the member galaxies is likely, the dispersion due to dust in these ellipticals must be smaller still.

Thus the HST color-magnitude diagram for each cluster hosting a SN provides an individual check for dust. NB: As long as we find a good tight red sequence on the color-mag diagram, it makes no difference if these clusters satisfy other criteria (e.g. X-ray) for a relaxed "official cluster". Our current data are already providing good constraints, but the proposed deeper color observations of many of the same clusters will allow us to improve these constraints close to the published red-sequence uncertainties. We can also use spectroscopic tests for dust and star for-

mation, since we have been obtaining multi-object spectroscopy for every cluster in our program, and every SN host in particular. This has allowed us to identify two elliptical hosts with [OII] emission (indicated by "C*" in Figure 1a). (Recent studies by Yan et al. (2006) indicate that most red ellipticals with [OII] match a quiescent elliptical without star formation or significant dust but apparently host LINERs, so these two SNe are likely to be brought out of "quarantine" if their hosts pass further tests. In our unbiased "blind analysis" approach they cannot be looked at on the Hubble diagram and dispersion analysis until we decide *first* if they do pass.)

Why is this cluster search much more efficient at finding and studying SNe Ia at $z \gtrsim 1$ than the previous HST searches in the GOODS fields? Not only does our program obtain $10\times$ the statistical weight per SN, but also per orbit: As reported in Figure 1, by searching in rich clusters we found and studied 10 elliptical-hosted SNe (7 in clusters) at $z \gtrsim 1$ (and 6 other SNe) using 219 orbits. For comparison, the GOODS searches in blank fields found and studied 6 elliptical hosted SNe at $z > 0.9$ (3 of these and 20 other SNe were at $z > 1$) using 674 orbits (Riess et al. 2007). One of our elliptical-hosted SN's lightcurve was not well observed (failed guide star), and two of the GOODS elliptical-hosted SNe were not well observed (first observation more than 20 days past peak). For this proposal, we will further increase our rate of elliptical-cluster-host SNe per orbit by over 60% by substituting newly-found rich clusters for the least-rich half of our cluster sample; none of our SNe were found in the latter (indicated by the gray region of Figure 3b). We will also increase the number of clusters searched (see below).

In addition to discovering more SNe Ia per HST orbit, there is another set of major efficiency gains in the *follow-up* of these SNe due to the knowledge of the host's elliptical morphology, the cluster redshift, and the higher rate per field. First, the follow-up observations need significantly less signal-to-noise ratio and fewer bands, since the extinction correction no longer dominates the requirements. Second, the higher discovery rate allows pre-scheduling observations for each cluster with a cadence guaranteed to sample well the lightcurves for every SNe discovered. This completely *eliminates the need for rapid-turnaround ToO* follow-up! Finally, these $z \gtrsim 1$ clusters' old stellar populations (Glazebrook et al. 2004, McCarthy et al. 2004) will overwhelmingly host SNe Ia, so much spectroscopy can be saved as well.

Determination of Cluster Masses with Weak Lensing

The number of clusters of galaxies as a function of mass and redshift provides a powerful alternative probe of the cosmology due to its sensitivity to the comoving volume *and* the growth of large scale structure. A number of large cluster surveys are now underway (e.g., SDSS, Red-Sequence Cluster Survey and Blanco Cosmology Survey) or imminent (e.g., South Pole Telescope Sunyaev-Zeldovich Survey, Dark Energy Survey) with this dark energy measurement as a key goal, but all require estimates for the cluster masses in order to successfully constrain cosmological parameters. In particular these surveys will need calibrations of mass-richness relations at $z \sim 1$ and will not be able to rely solely on low redshift calibrations. Weak gravitational lensing of background galaxies is now a well-established technique for providing a *direct* measurement of the projected cluster mass, without any assumptions about the makeup or dynamical state of the cluster. The weak-lensing observations proposed here will provide the most accurate calibration of the masses of high redshift clusters for years to come and will serve as the necessary reference to ensure that the next generation cluster surveys can reliably use clusters beyond $z \sim 1$ to constrain

w to better than $5-10\%$. The recent work of Majumdar & Mohr (2003, 2004) on "self-calibration" shows that detailed study of only a moderate sample of clusters (such as that proposed here) can reach those goals.

The redshift evolution of the mass function of clusters provides different cosmological information from the mass function at low redshift. In particular it breaks the degeneracy between σ_8 and Ω_m (Bahcall & Bode 2003). Our results will tie down the high redshift $z = 1 - 1.5$ range, while the SDSS MaxBCG group has measured the mass richness relation to similar accuracy at $z \approx 0.1 - 0.3$ (Johnston et al. 2007), so that together cluster masses can be calibrated and compared all the way from z=0 to z=1.5. The improved accuracy in the mass measurements also allows us to better quantify the scatter (an often ignored, but critical part of cluster abundance studies) in these relations much better (Gladders et al. 2007).

We have completed a preliminary weak lensing analysis of the Cycle 14 data. A plot of the mass-richness relation is shown in Figure 3b. These data can constrain the zero point of the mass richness relation to about the 25% level. In place of our less-rich clusters (ranked in the lower half of our current sample, indicated in gray in Figure 3b), we will substitute newly discovered richer clusters from our ongoing discovery surveys (e.g. RCS- 2). This will allow for higher signal-to-noise ratio mass measurements and add more dynamic range on our mass-richness plot which will help to better constrain the slope of this relation. The additional Cycle 16 color data for the clusters that we continue to follow will also increase the effective number density of useful sources from ~ 100 to ~ 150 arcmin^{-2}. This improvement in depth combined with the higher average mass will reduce the uncertainty in individual masses to 23% for the average cluster in our sample ($M = 3 \times 10^{14} M_\odot$ including the new clusters) and will reduce the error in the zero point of the mass richness relation to the 12% level. The current uncertainty in mass estimates, due to the disparity among other estimators (X-ray, dynamical etc), is at least 30% and so this improvement will allow for new and interesting constraints.

Strong lenses at $z \gtrsim 1$. The image quality provided by the ACS dramatically increases the number of faint, low surface brightness strongly lensed arcs and image families detectable – particularly with the use of multicolor data we propose for in Cycle 16. Our Cycle 14 cluster sample included 8 clusters with giant arcs, nearly all of which lie behind the richer half of our clusters. Based on our statistics from Cycle 14, we expect the proposed observations to increase this number to 12 lensing clusters. Previously, only a single $z \gtrsim 1$ lensing cluster had been imaged by the HST. Each arc in a high redshift cluster measures the mass interior to its position (typical Einstein radii are ~ 100 kpc/h). When combined with our complementary larger scale (~ 1 Mpc/h) weak lensing analysis, strong lensing information improves our cluster mass estimates and provides leverage on the mass profiles of the clusters (i.e. concentration parameters), testing for $z \gtrsim 1$ dark matter halos for the first time.

Galaxy Cluster Science at $z \gtrsim 1$

Whether they form via monolithic collapse (Eggen, Lynden-Bell & Sandage 1962) or hierarchical assembly (White & Frenk 1991), massive elliptical galaxies account for a substantial fraction of the stellar mass in the Universe (Hogg et al. 2002), and are found in highly overdense regions (Dressler 1980; Hogg et al. 2003) - i.e., galaxy clusters. The slope, scatter, and intercept of the cluster elliptical galaxy color magnitude relation at $z < 1$ are surprisingly well matched

by a simple star formation history consisting of a burst at $z > 3$ followed by passive evolution (Stanford et al. 1998), and their luminosity functions also are fit by such models (de Propris et al. 1999). ACS imaging of more distant clusters will determine how far this scenario can be pushed, by enabling measurements of the merger and elliptical fractions, their luminosity functions – and new in this proposal – precise measurements of the color-magnitude relation (CMR).

Postman et al. (2005) use morphological analyses of ACS GTO imaging of 7 clusters ($0.8<z<1.3$) to show that the fraction of ellipticals at a given density does not change up to $z\sim1.25$, and that the fraction of S0s remains roughly constant at the 20% level seen in $0.4 < z < 0.5$ clusters. Hence, the formation of all massive cluster ellipticals, and a significant fraction of the lenticulars as well, must be occurring at $z > 1.25$. This is supported by limits on the most recent star formation from the small dispersion and lack of evolution of the CMR's out to $z \gtrsim 1$ (see Figure 3a).

This proposal takes the next step beyond the existing small sample and upper redshift to probe the regime in which massive cluster galaxies are being formed. The GTO program has three clusters at $z > 1$, while our sample will have 35 after Cycle 16. The highest redshift of the clusters is pushed from $z = 1.27$ to $z = 1.5$. Moreover, the addition of Cycle 16 images will vastly improve measurements of the mean and dispersion of the CMR, limiting the time of the most recent epoch of star formation. In conjunction with data we have obtained from Chandra, XMM, Keck, Subaru, the VLT, Magellan, and Spitzer, the ACS data to be obtained in this proposal will determine the epochs of the assembly of ellipticals and the origin of S0s, and calibrate the relation between mass and X-ray luminosity and temperature (and future SZ mass determinations) at these redshifts.

Supernovae rates. The rate of SNe in $z \gtrsim 1$ galaxy clusters will address several outstanding questions about the intracluster medium (ICM), as well as providing important constraints on SN Ia progenitor scenarios: (1) The first high-significance test of the proposal that the cluster Ia rate was much higher in the past, accounting for the unexplained high metallicity in the ICM (Brighenti & Mathews 1999, Pipino et al. 2002, Matteucci et al. 2006). (2) Constraints on the fraction of "hostless" SNe in the clusters (at the $\sim 5-7$ % level) will provide the first direct estimate of the fraction of stars in unobservable low-surface-brightness populations in the ICM. (3) Comparison with similar galaxy cluster SN rate measurements at low and intermediate redshift (Sharon et al. 2006a, 2006b) 2006b=intemediate z by NS) will provide important constraints on Type Ia progenitor models (Mannucci et al. 2006, Sullivan et al. 2006). Our program will bring the sample size of cluster ellipticals to a level needed to address these questions.

Conclusions

The observations proposed capitalize on our new approach to high-redshift SNe measurements and will provide a first robust measurement, unbiased by extinction correction, of w_0 vs. w' and of $w(z > 1)$. They will then comprise a springboard for a wide array of astrophysical investigations: high redshift SNe, cluster profiles, gravitational lensing, and multiwavelength studies of large scale structure and cosmology. The emphasis on high redshift and attention to systematics is essential for bringing to maturity key next-generation cosmological techniques, while the cluster data will serve as a bedrock scientific legacy for extragalactic astronomy.

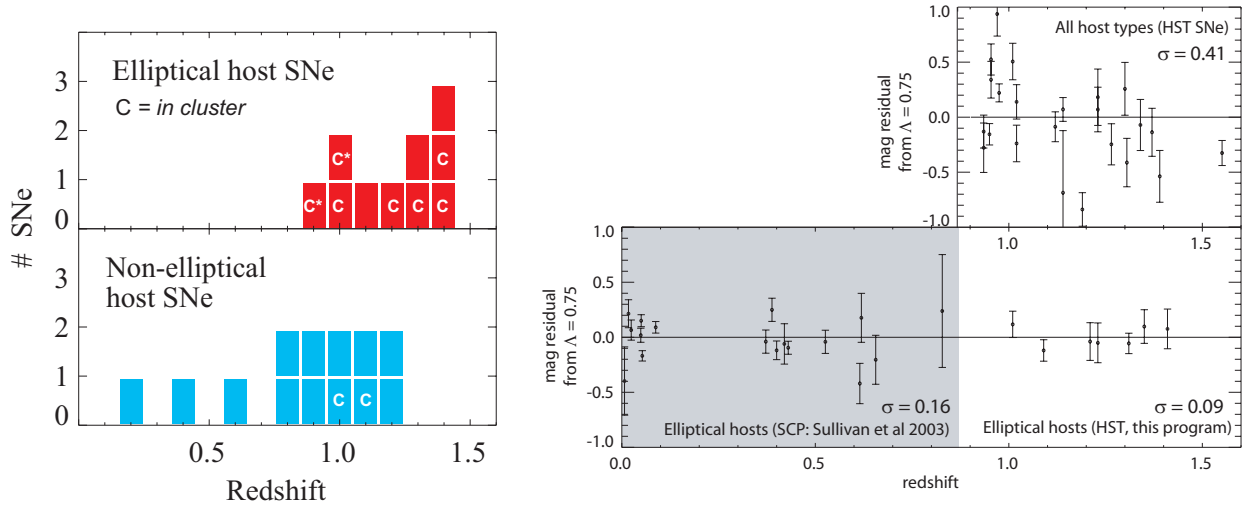

Figure 1: **(a) Left Panel:** The redshift distribution of the SNe discovered in our Cycle 14 program. The upper panel shows the distribution of elliptical galaxies that had SNe Ia, with the cluster members indicated by "C". The asterisk indicates OII emission in the galaxy spectrum; there is evidence (see text) that these may be quiescent red galaxy environments, so after further tests these SNe may yet be included on the cluster-ellipticals SN Hubble diagram. The lower panel shows the distribution for non-elliptical hosts. Not shown are an additional ten SNe with good lightcurves, but so far without redshifts because the host galaxy was very unlikely to pass our redshift-range and ellipticals-only cuts. **(b) Right Panel:** The Hubble diagram, plotted as a residual from a flat $\Omega_\Lambda = 0.75$ universe, for (upper panel) the whole Riess et al. 2007 $z > 1$ sample, and for (lower panel) Elliptical-host-only SNe Ia from SCP (Sullivan et al. 2003) and from preliminary analysis of our Cycle 14 SNe (not shown: "C*" from Fig. 1 and the SN lost to guide-star failure). The measured dispersion, $\sigma = 0.41$ mag, for the mixture of SNe Ia in all host types (upper panel) reanalyzed with an extinction correction, shows the dramatic increase in error bars due to the large uncertainty in $B - V$ color at $z > 1$ being multiplied by $R_B \approx 4$; this is compounded by the uncertainty in R_B and intrinsic color, and any drift with redshift. The ratio of this $z > 1$ dispersion to the elliptical-hosted $z > 1$ dispersion of bottom-right panel makes the elliptical-hosted SNe each worth more than 10 of the extinction-corrected others.

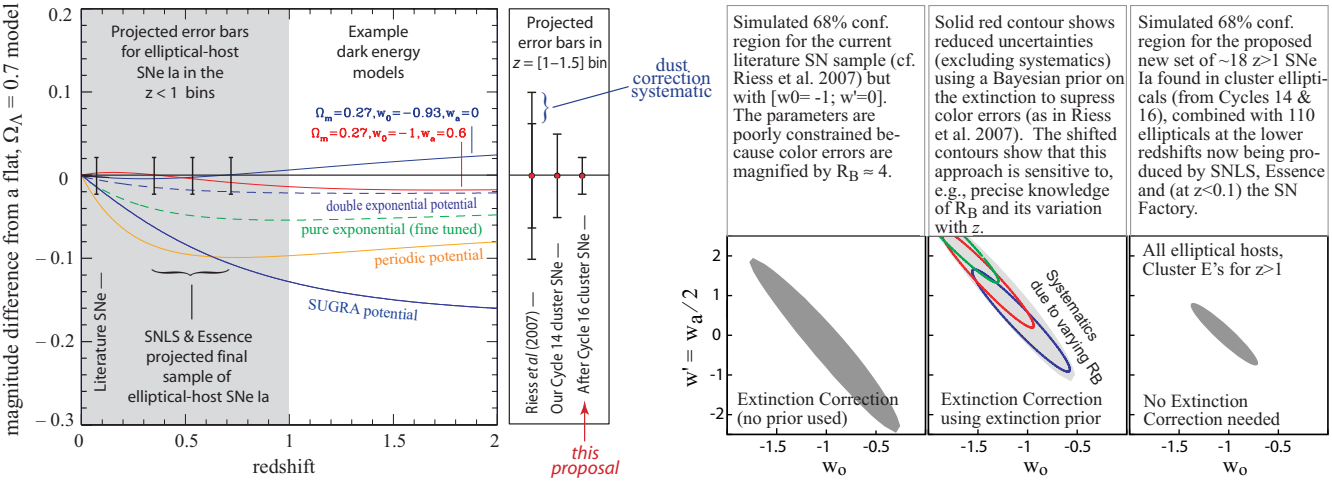

Figure 2: **(a) Left Panel:** Hubble diagram residuals from Λ cosmology for several example dark energy models compared with the projected redshift-binned error bars expected from this project and current large projects finding SNe Ia in elliptical hosts. The ground-based projects should obtain the binned error bars shown at redshifts $z < 1$. The $z = [1 - 1.5]$ bin needs HST observations: The 23 SNe Ia from GOODS searches (Riess et al. 2007) yield a binned statistical uncertainty (~ 0.06 mag) somewhat larger than estimated for the 5 cluster-elliptical-host SNe from our just-completed Cycle 14 search. However, the extra dust-correction systematic error is significant for non-elliptical-host SNe. The projected error bar after adding the proposed Cycle 16 cluster-elliptical-host SNe is 0.022 mag, based on 18 total SNe and extra orbits to improve the SN's photon noise. **(b) Right Panel:** Schematic explanation of the difference between the $w_0 - w'$ confidence regions expected from conventional SN Ia Hubble diagrams and from cluster-elliptical-host SNe Ia.

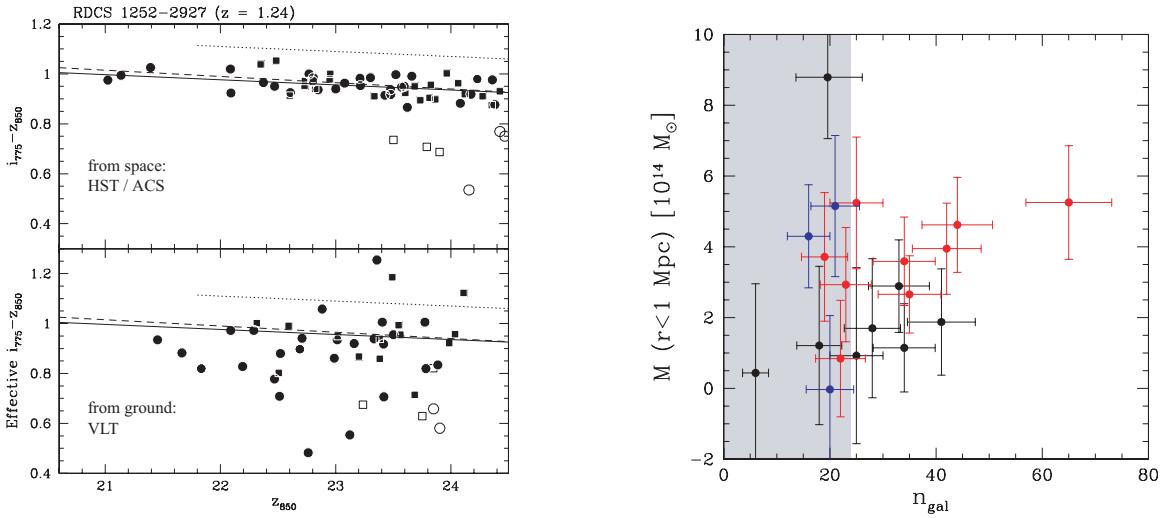

Figure 3: **(a) Left Panel:** The dust-free nature of cluster ellipticals (circles) in RDCS 1252-2927 at $z = 1.24$ is supported by the small scatter of the color-magnitude relation (CMR) when ACS quality photometry is used (from Blakeslee et al. 2003). The CMR in this same cluster using data from the VLT FORS and ISAAC (transformed to the ACS i,z passbands) exhibits nearly 8 times the scatter, demonstrating the need for HST imaging. With this large ground-based scatter, the outliers from the space-based CMR (indicated by open symbols) cannot be distinguished. **(b) Right Panel:** Weak lensing mass versus the estimated number of early type cluster members based on a preliminary analysis of our Cycle 14 data. The lensing masses were determined from a fit to the tangential shear. The $n_{\rm gal}$ parameter is an estimate of number of early type cluster galaxies in the ACS FOV. Objects with a color (i_{775} - z_{850}) within 0.1 mag of the cluster red-sequence are counted after identifying early type galaxies using a simple concentration parameter. Future analysis will include a cluster richness parameter accounting for the luminsity-redshift relation. The black points indicate clusters from the IRAC survey, red points from RCS and blue points from RDCS. The clusters that hosted SNe were all in the unshaded (higher richness) region. Note that, because of the high redshifts of the clusters, outliers at the low richness end are expected.

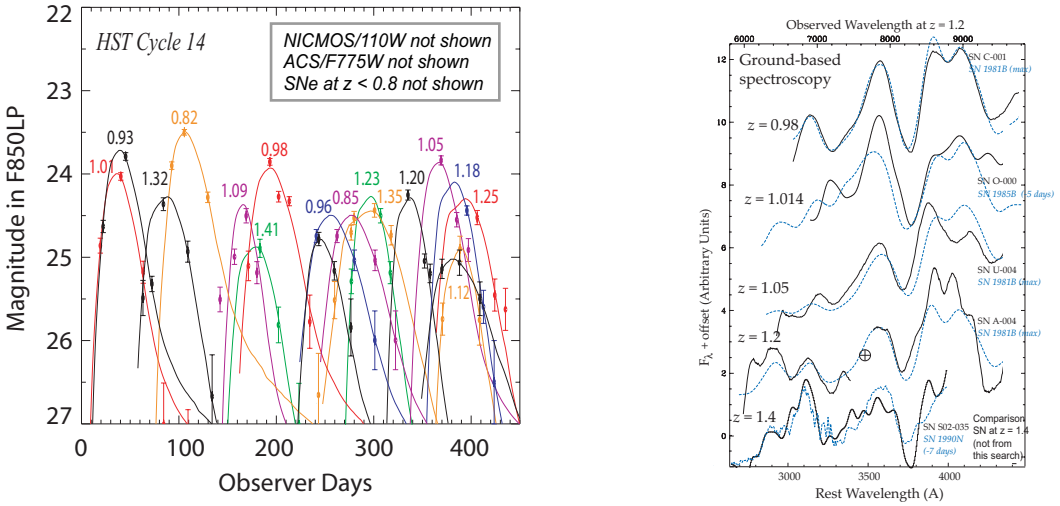

Figure 4: **(a) Left Panel: (a) Left Panel:** Preliminary lightcurves of a subset of the SNe discovered in Cycle 14, demonstrating the repeat cadence on each cluster that results in following every SN in the field with typical fit peak magnitude total uncertainties of 0.07 to 0.15 mag. **(b): Right Panel:** Ground-based spectra (VLT, Keck, Subaru) for SNe Ia discovered in our cycle 14 program (solid curves) de-redshifted to the SN restframe. Host galaxy light has been removed and a low-pass filter applied to remove features with widths narrower than that of a SN. One spectrum obtained in previous SCP SN campaigns is also shown to demonstrate ground-based spectroscopy out to z=1.4. For each spectrum, a matching template spectrum from a well-studied nearby SN is shown (dashed curves).

Description of the Observations

The supernova observing strategy

We implement three improvements over our observing strategy in Cycle 14: (1) we increase the number of clusters from 22 to 27 (23% increase in number of cluster SNe) and replace the poorer clusters in the original sample with much richer clusters ($\sim 60\%$ increase in number of cluster SNe), (2) upon discovery of a valuable elliptical hosted SN, we will schedule an additional 1-2 (depending on the redshift of the SN) ACS visits to supplement the observing cadence ($\sim 30\%$ increase in SNR), and (3) we will produce deeper references for SNe discovered in both programs ($\sim 25\%$ increase in SNR for SNe with deep references).

The high rate of SNe Ia produced in clusters *in addition* to the SNe Ia in the fore/background field galaxies makes possible an elegantly simple combined search-and-follow-up scheduling strategy, which we successfully demonstrated in Cycle 14. We observe each cluster for one orbit every ∼21-24 days for ∼8 visits, where the exact cadence depends on the cluster redshift and the exact number of visits depends on HST observing constraints. Every SN that appears in these clusters and fields, modulo small end effects, has a fully sampled lightcurve in two bands (each orbit contains four ACS/F850LP dithered cosmic-ray splits plus one, longer ACS/F775W exposure)—without the need for expensive Target of Opportunity (ToO) observations (see Fig. 4a). We obtain ground-based spectroscopy for precise redshifts and confirmation of elliptical galaxy type (which confirms SN Ia identification), and/or a spectrum of the SN itself (Fig. 4b). We always discover the SN early enough (Fig. 4a) that we can use a (>2-week-advance-notice) low impact ToO for additional NIC2 F110W observations within ±5 days of the SN lightcurve peak for all SNe above $z > 1$. Only for the highest redshift SNe Ia $z > 1.4$ is a full 7-orbit lightcurve with NIC2 F110W taken. (NICMOS fields are too small to be used in the search.)

We use the F775W-F850LP color to correct field-galaxy SNe for extinction, and both F850LP-F110W and F775W-F850LP colors to study intrinsic colors – and its possible relation to luminosity – for SNe in cluster and field elliptical hosts (which will greatly help the calibration of the GOODS SNe). For $z \lesssim 1.25$, these are B-V and U-B restframe colors, and for $z \gtrsim 1.25$ these are U-B and a UV color (less useful, but free). The fluxes/magnitudes, cadence and error bars shown in Fig. 4a demonstrate the SNR obtained with the cadence and exposure times from Cycle 14. The improvements in the Cycle 16 observing strategy will result in twice as many SNe hosted by cluster ellipticals, and with a distance modulus uncertainty below ∼0.07 mag. This improved measurement will significantly improve cosmological constraints in this important redshift range and will allow for a detailed study of the new-found small intrinsic dispersion of this class of SNe.

In summary, we require 188 pre-scheduled ACS orbits along with 18 ACS orbits used to improve lightcurve coverage, as well as 28 ToO orbits for the observation of 14 SNe using NIC2 F110W (10 single-orbit ToOs for SNe with $1 \lesssim z \lesssim 1.25$; two 2-orbit observations for SNe with $1.25 \lesssim z \lesssim 1.35$; and two 7-orbit sequence ToO scheduled over approximately 6 weeks needed to obtain the restframe B lightcurve for the SNe at $z \gtrsim 1.35$). ACS is the best instrument for this program (even better than WFC3).

Utilizing deep references images:

For ∼2 of the SNe observed with NICMOS we expect the SN to be close to the core of a bright

host, requiring an additional final image after the SNe has faded with a 3-orbit depth so as not to degrade the signal-to-noise ratio after subtraction. Offsetting this requirement for 6 additional orbits is the probability of canceling the final two cadence observations for clusters that have not produced a SNe in time to be followed for sufficient lightcurve points. This happens often enough (and 3 weeks in advance) that we can reschedule these canceled final observations to provide the post-SNe visit for the cases that require them without major scheduling complications.

Spectroscopic identification and redshift determination: Our team has been running large ground-based programs at Subaru (≈10 half-nights per semester), VLT (≈16 hours queue time), Keck (≈2 nights per semester), and Magellan (≈10.5 nights per semester), providing host galaxy and/or SNe spectra for every one of the SNe discovered in the program. (Fig. 4a shows that some of our SNe are always observable.) The host spectra confirm redshift and elliptical identity for every host – thus confirming Type Ia status for those without a "live" spectrum. Note that this host galaxy data is sufficient to give >90% confidence that we have identified a Type Ia; this is comparable to the success rate with spectroscopic ID's at these redshifts (from ground or HST). Fig. 4b shows that ground-based spectra for SNe Ia at redshifts as high as $z \sim 1.4$ are able to identify the SNe comparably to ACS/grism. (Fig. 4b shows several SN spectra from Cycle 14 SN. Not shown are host galaxy spectra for *all* the Cycle 14 SNe.) At still higher redshifts the ACS/grism can occasionally obtain a usable spectrum, but at a cost of over 12 orbits. This is unnecessary for SNe in a well-confirmed cluster elliptical host, and for a possibly dusty spiral we would rather use the same number of orbits to find a new –much more useful – elliptical-hosted SN!

Observing requirements for the cluster science

The observational requirements for the cluster science are driven by the goals associated with characterizing the formation and evolution of the cluster galaxies. These requirements include **(1)** obtaining reliable morphological classifications (performed both visually and via machine algorithms) to 2 magnitudes below L^* at $z \sim 1.2$ (~ 24 AB mag in 850LP) using the standard system of elliptical, lenticular, and spiral/irregular over an area reaching out to r_{200}, **(2)** measurement of the slope and intercept of, and intrinsic scatter about, the early-type red sequence to a precision of $\lesssim 20\%$ and **(3)** deriving galaxy effective radii with sufficient accuracy to enable estimates of M/L ratios for early-type galaxies when coupled with velocity dispersions from on-going ground-based programs. Goal (1) requires an integrated S/N $\gtrsim 25$ over the central 10 kpc of the galaxy; Goal (2) requires colors with uncertainties $\lesssim 0.01$ mag at the above classification limit (24 AB mag) – this requirement is driven by the small scatter (∼0.025 mag) already observed at these redshifts and Goal (3) is well satisfied by the constraint imposed by the first two. From data already in hand we determine that the S/N of photometry for galaxies with AB mag ≤ 24 will meet or beat all these requirements. The list of targeted clusters is based on the richest clusters observed in Cycle 14. With high redshift cluster searches currently ongoing (RCS-2, XMM, IRAC) we have substituted recently discovered rich clusters, replacing the poorer half of the original sample. We may also find additional rich substitutes before Phase II.

Observing requirements for the weak lensing studies

To compute the accuracy with which we can determine the masses of clusters we used data from the UDF to determine the "effective" number density of sources used in the lensing analysis.

These estimates include a proper weighting for the smaller sources which have sizes comparable to the PSF. We find excellent agreement when these numbers are compared to the results obtained with clusters already observed. The proposed exposure times give similar source densities in both filters and, combining measurements in both filters, yields the estimated accuracy in mass determination given above in the Scientific Justification. These calculations also agree well with published results (Jee et al. 2005, 2006; Lombardi et al. 2005). Our detailed calculations show that the gain from mosaicing is minimal for clusters beyond $z = 1$ and that it is instead deeper observations that provide more accurate masses.

Special Requirements

The 27 galaxy clusters in this proposal are each visible for at least three months during Cycle 16. The search for SNe is most efficient when this full visibility window is utilized with new observations every 20-26 days. The timing of the cluster visibility windows requires a few months of overlap with the following cycle in order to complete the SN search for 4 clusters in the sample. The first cluster is visible July 2, the very beginning of the observing cycle, and the last cluster disappears on Sept 23, 2008. We swap in an equivalent cluster if a cluster does not schedule well. The total request is 206 ACS orbits and 28 NICMOS orbits over a period of 448 days.

In association with the >2-week-advance-notice NICMOS ToO's, we request 28 orbits of Coordinated Parallel ACS observations to be used in conjunction with the data from the wider field surveys from which the clusters were discovered.

Coordinated Observations

Justify Duplications

Every proposed observation will search for, or follow-up, new SNe. Previous ACS observations of these targets will provide deeper reference images, important help for the SN search.

References

⊙ Bahcall, N. & Bode, P., 2003, ApJ, 588, L1 ⊙ Barbary, K. et al. 2006, AAS, 209, 90.01 ⊙ Blakeslee, J. et al. 2003, ApJL, 596, 143 ⊙ Bower, R. et al. 1992, MNRAS, 254, 589 ⊙ Brighenti, F. & Mathews, W. 1999, ApJ, 515, 542 ⊙ Dawson, K., et al. in prep. ⊙ De Propris, R. et al.1999, AJ, 118, 719 ⊙ Draine, B. 2003, ARA&A 41, 241 ⊙ Dressler, A. 1980, ApJ, 236, 351 ⊙ Eggen, O. et al. 1962, ApJ, 136, 748 ⊙ Ellis, R. et al. 1997, ApJ, 483, 582 ⊙ Gladders, M. et al. 2007, ApJ, 655, 128 ⊙ Glazebrook, K. et al. 2004, Nature, 430, 181 ⊙ Hogg, D. et al.2002, AJ, 124, 646 ⊙ Hogg, D. et al.2003, ApJ, 585, 5 ⊙ Hogg, D. et al. 2004, ApJ, 601, 29 ⊙ Jha, S. et al. 2007, ApJ, accepted ⊙ Jee, M. et al. 2005, ApJ, 618, 46 ⊙ Jee, M. et al. 2006, ApJ, 642, 720 ⊙ Johnston, D. et al. 2007, in press ⊙ Knop, R. et al. 2003, ApJ, 598, 102 ⊙ Lombardi, M. et al.2005, ApJ, 623, 42L ⊙ Majumdar, S. & Mohr, J. 2003, ApJ, 586, 603 ⊙ Majumdar, S. & Mohr, J. 2004, ApJ, 613, 41 ⊙ Mannucci, F., et al. 2006, MNRAS, 370, 773 ⊙ Matteucci, F., et al. 2006, MNRAS, 372, 265 ⊙ McCarthy, P. et al. 2004, ApJ, 614, L9 ⊙ Pasquali, A et al. 2006, ApJ, 636, 115 ⊙ Perlmutter, S. et al. 1999, ApJ, 517, 565 ⊙ Pipino, A. et al. 2002, NewA, 7, 227 ⊙ Postman, M. et al. 2005, ApJ, 623, 721 ⊙ Riess, A. et al. 2004, ApJ, 607, 665 ⊙ Riess, A. et al. 2007, ApJ in press ⊙ Sharon, K. et al. 2006a, astroph/0610228 ⊙ Sharon, K. et al. 2006b, astroph/0611920 ⊙ Stanford, S. et al. 1998, ApJ, 492, 461 ⊙ Sullivan, M. et al. 2003, MNRAS, 340, 1057 ⊙ Sullivan, M. et al. 2006, ApJ, 648, 868 ⊙ Temi, P. et al. 2005, ApJ, 635, L25 ⊙ Tran, H. D. et al. 2001, AJ, 121, 2928 ⊙ van Dokkum, P. et al. 2001, ApJ, 552, 101 ⊙ White, S. & Frenk, C. 1991, ApJ, 379, 52 ⊙ Yan, R., 2006 ApJ, 648, 281